



# Performance and autopsy of nanofiltration membranes at an oil-field wastewater desalination plant

Dongsheng Zhao<sup>1</sup> · Chang Su<sup>1</sup> · Guicai Liu<sup>2</sup> · Youbing Zhu<sup>3</sup> · Zhengyang Gu<sup>3</sup>

Received: 28 May 2018 / Accepted: 19 November 2018 / Published online: 27 November 2018  
© Springer-Verlag GmbH Germany, part of Springer Nature 2018

## Abstract

In this study, the long-term operational performance of an on-site NF facility at a full-scale oil-field wastewater desalination plant was monitored. The NF facility with poor permeability due to membrane fouling enables efficient multivalent salt removal (rejections of  $Mg^{2+}$ ,  $Ca^{2+}$ ,  $Fe^{3+}$ , and  $Al^{3+}$  were approximately 100%). Moreover, a comparison of the cleaning efficiencies of two on-site cleaning modes indicated that PL-007 cleaning helped to improve the effectiveness of subsequent acid cleaning in the removal of inorganic foulants. Furthermore, a spiral-wound NF membrane module harvested from the plant was unfolded and autopsied. The results showed that both anionic polyacrylamide (APAM) and crude oil were identified as the predominant organic matter on the membrane surface and collectively accounted for a substantial fraction (86.3%) in terms of dry weight. Additionally, dissolved organics with a high molecular weight were prone to accumulation on the membrane surface. Multivalent elements, including Mg, Ca, Al, Fe, and Si, were the primary inorganic species in the fouling layer. Among the inorganic elements, Si occupied a high proportion and existed in the form of  $SiO_2$  in the fouling layer. According to the autopsy results, organic fouling combined with inorganics was responsible for the decline in the flux.

**Keywords** Nanofiltration · Oil-field wastewater · Performance · Fouling · Cleaning

## Introduction

The importance of petroleum to modern civilizations is well known. Most of China's oil fields (such as the Shengli and Daqing oil fields) have already entered their middle or late periods of production. The application of polymer (i.e., anionic polyacrylamide (APAM)) flooding technology in oil fields has effectively improved crude oil

recovery (Li et al. 2017, Riahi-zhad et al. 2017), but the large amount of clean-water consumption and wastewater output during this process has raised severe water-shortage concerns. The production of APAM-containing wastewater is as high as 5 million tons each year (Liu et al. 2016a). Due to relatively high water flux and the rejection of dissolved solids, organics, and colloidal matter, the nanofiltration (NF) process has been deemed a promising technology to efficiently reduce mineralization and to remove the organic residuals (to meet the quality requirements) in oil-field wastewater (Alzahrani et al. 2013, Cakmakci et al. 2008, Mondal & Wickramasinghe 2008, Zhang et al. 2015). Reusing this wastewater to prepare the polymer solution is expected to solve the economic and environmental problems caused by clean-water consumption and wastewater discharge.

As in other membrane-based separation processes (e.g., ultrafiltration (UF) (Liu et al. 2016b, Wang et al. 2014), electrodialysis (ED) (Guo et al. 2015), and forward osmosis (Han et al. 2015, Phuntsho et al. 2014), fouling is a major issue restricting the efficient operation of NF facilities and can cause the membrane performance to deteriorate, as well as increasing the operational costs (Li & Elimelech 2004). Foulants can be classed into four major categories: inorganic scale, colloidal or

---

Responsible editor: Angeles Blanco

**Electronic supplementary material** The online version of this article (<https://doi.org/10.1007/s11356-018-3797-x>) contains supplementary material, which is available to authorized users.

---

✉ Dongsheng Zhao  
zds123123@yeah.net

<sup>1</sup> College of Civil Engineering and Architecture, Nanyang Normal University, Nanyang 473061, China

<sup>2</sup> School of Civil Engineering and Architecture, University of Jinan, Jinan 250022, China

<sup>3</sup> State Key Laboratory of Pollution Control and Resources Reuse, School of Environmental Science and Engineering, Tongji University, Shanghai 200092, China

particulate matter, organic substances, and microorganisms. Inorganic scale formation in membrane systems has been reported to occur by a combination of two extreme mechanisms: surface crystallization and bulk crystallization (Antony et al. 2011). Colloidal and particulate matter rejected by the membrane may form a dense fouling layer, resulting in additional resistance to filtration. Organic fouling is dominated in part by the interactions between the organic foulants and the membrane surface, as well as among the organic foulants themselves. Microbial attachment and growth on the membrane surface result in the formation of biofilms, which consist of microbial cells embedded in an extracellular polymeric substance matrix. Although great efforts have been made to mitigate membrane fouling, including feed water pretreatment (Gur-Reznik et al. 2008, Lai et al. 2013, Ohno et al. 2010), operational parameter optimization (Ochando-Pulido et al. 2012), and membrane surface modification (Asatekin & Mayes 2009, Kang & Cao 2012, Zhao et al. 2014, Zhao & Ho 2014), fouling is still inevitable.

To better understand the physico-chemical processes governing fouling, autopsies of fouled membranes have been performed. Various analytical methods, including inductively coupled plasma mass spectrometry (ICP-MS), gas chromatography/mass spectrometry (GC-MS), Fourier transform infrared spectroscopy (FTIR), and X-ray diffraction (XRD), have been employed to identify the major foulants on the membrane surface. Nevertheless, different source water qualities result in diverse fouling scenarios (Khan et al. 2013). For instance, it has been reported that there were significant differences in the compositions of the fouling layers of membranes for wastewater reuse and seawater desalination (Khan et al. 2014). For NF membranes treating oil-field wastewater (Fletcher et al. 2015) that contains complex components of organic and inorganic substances (Guo et al. 2015, Liu et al. 2016b), few studies have focused on the identification of the foulants. Accordingly, to provide fundamental evidence for the analysis of reasonable fouling mechanisms, extensive characterizations and chemical analyses of NF membranes fouled by oil-field water were conducted in this study.

The specific objectives of the study were as follows: (1) to monitor the long-term performance of an NF facility in a full-scale oil-field wastewater desalination plant, (2) to compare the cleaning efficiencies of the two on-site cleaning modes, (3) to identify the main compositions of the foulants on the fouled NF membrane surface, and (4) to propose the potential fouling mechanisms of NF membranes in oil-field wastewater treatment. The results obtained in the study are promising for prediction and controlling the fouling of NF membranes during oil-field wastewater desalination.

## Materials and methods

### Description of the full-scale plant and NF facility

The full-scale plant is located at the Daqing oil field in China, has a design capacity of 9800 m<sup>3</sup>/d for oil-field wastewater desalination, and consists of a biological pretreatment unit, a UF unit, an ED unit, and an NF unit. The detailed process flow diagram of the plant is shown in Fig. S1.

The primary function of the NF facility (Fig. 1) is to recycle the ED concentrate in order to improve the water production rate of the integrated membrane system. The NF facility is capable of producing 1350 m<sup>3</sup>/d of permeate and includes a concentrate recycle stream to improve the recovery up to 75%. The flux decline is significant, and the original aim of operating at 75% recovery is not possible due to membrane fouling. Even after frequent chemical cleaning (once every 3 days), the NF facility can only operate at 25% recovery at best. In this study, the fouled NF membrane module selected for the autopsy and cleaning tests had been in operation for approximately 3 year.

Prior to entering the NF facility, the ED concentrate is amended with antiscalant and filtered through a 5 µm-pore-size cartridge filter. The applied feed pressure of the NF facility is approximately 1.5 MPa. The facility was designed with a typical configuration of two stages in series, housing five membrane modules (Sepro, NF-1, USA) per pressure vessel. In total, the NF facility includes 150 membrane modules. A summary of the characteristics of the NF-1 membrane (Kumar & Pal 2014) is listed in Table 1.

Chemical cleaning at the NF facility is performed once every 3 days. First, the membrane modules are flushed with 0.5% hydrochloric acid solution, after which the modules are soaked for 90 min in the solution. Afterwards, the membrane modules are flushed with PL-007 (a commercial cleaning agent containing alkaline and anionic surfactant) and then soaked for 90 min with the cleaning agent. The maximum feed pressure applied during CIP operation is 0.6 MPa. Finally, the facility is flushed (from the feed side) with permeate twice before returning to operation.

### Water quality characterization

The feed and permeate of the NF facility were analyzed through measurements of pH, conductivity, and total dissolved solids (TDS). The concentrations of cationic ions and silicon were analyzed by inductively coupled plasma optical emission spectrometry (ICP-OES, Agilent 720ES, USA). Bicarbonate and carbonate were determined using acid-base titration. The chloride level was measured by silver nitrate titration methods. The crude oil content was quantified by UV spectrophotometry, and the anionic polyacrylamide (APAM) concentration was determined using the starch-

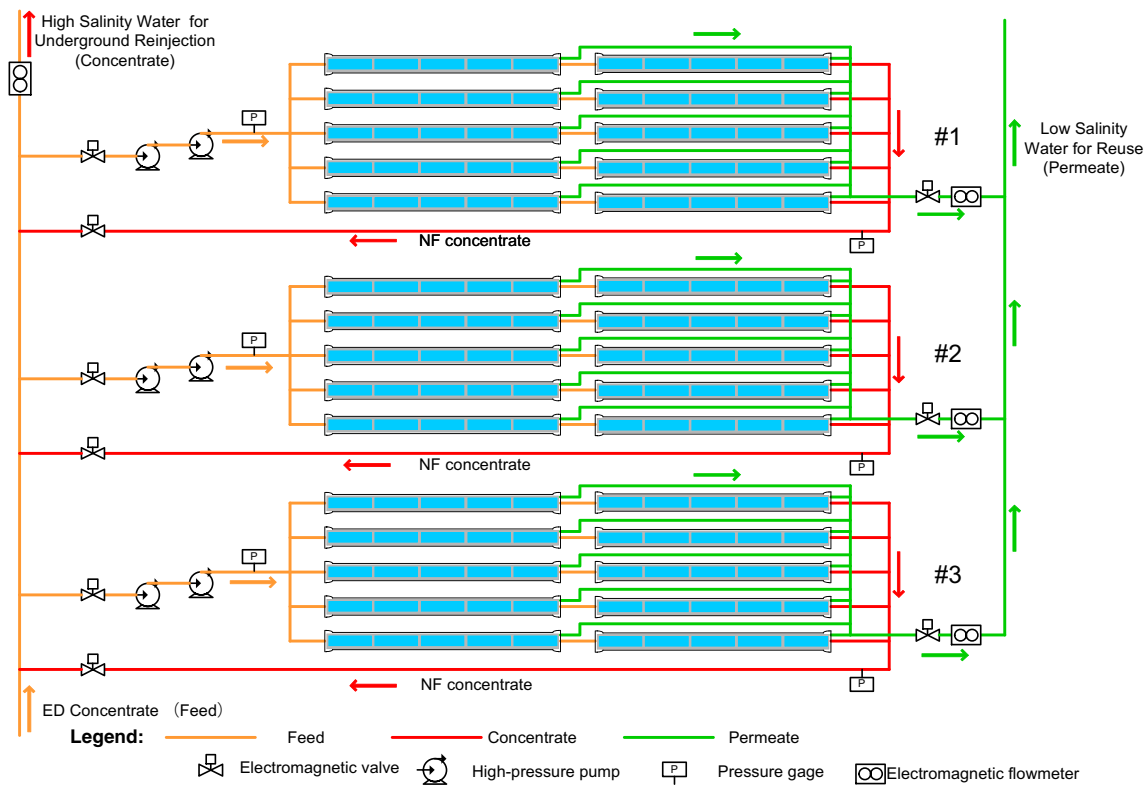


Fig. 1 Schematic diagram of the NF facility

triiodide method (Guo et al. 2015). The chemical structure of the APAM is presented in Fig. S2. The water quality parameters of the feed and permeate are listed in Table 2.

### Autopsies of fouled NF membranes

The acquired membrane module was sawed using a hacksaw and then unfolded. The membrane sheets were then kept at 4 °C in the dark until further analysis.

### Scanning electron microscopy (SEM) energy dispersive X-ray (EDX) analyses

The morphologies and element compositions of the fouled NF membranes were examined via SEM-EDX analysis (XL30FEG, Philips, Netherlands). For the cross-section analyses, liquid nitrogen was initially employed to fracture the membrane sheets. The membrane sheets were then sputtered with a thin layer of gold prior to measurement.

**Table 1** Summary of the characteristics of the NF-1 membrane (Kumar & Pal 2014)

Items	NF-1
Composition of the top layer <sup>a</sup>	Fully aromatic polyamide
MWCO (Da) <sup>a</sup>	150–250
Pore size (nm) <sup>a</sup>	0.53
Rejection of NaCl (%) <sup>b</sup>	90.0
Rejection of MgSO <sub>4</sub> (%) <sup>b</sup>	99.5
Maximum clean-in-place (CIP) temperature (°C) <sup>a</sup>	50
Maximum applied pressure (bar) <sup>a</sup>	45
CIP pH limitation <sup>a</sup>	2–12

<sup>a</sup> According to the manufactures

<sup>b</sup> Test conditions: feed pressure of 1.03 MPa, NaCl concentration of 2000 mg/L, MgSO<sub>4</sub> concentration of 2000 mg/L, and temperature of 25 °C

**Table 2** Water quality of the feed and permeate of the NF facility

Parameters	Feed	Permeate
pH	8.67–8.74	7.68–7.84
TDS (mg/L)	5385.8–6767.1	203.9–358.6
Na (mg/L)	1276.9–1893.9	55.0–87.2
Mg (mg/L)	5.6–7.7	–
Ca (mg/L)	13.1–15.6	–
Fe (mg/L)	0.45–0.83	–
Al (mg/L)	0.08–0.21	–
Si (mg/L)	9.14–9.48	–
Cl <sup>−</sup> (mg/L)	1024.7–1219.6	61.9–85.0
HCO <sub>3</sub> <sup>−</sup> (mg/L)	2745.0–3239.1	82.4–189.1
CO <sub>3</sub> <sup>2−</sup> (mg/L)	252.2–336.0	–
APAM (mg/L)	101.1–117.9	–
Crude oil (mg/L)	0.53–0.64	0.25–0.31

The ranges are shown for seven randomly collected water samples

### Fouling load analyses

Foulants were collected from a measured surface area (approximately 400 cm<sup>2</sup>, performed in triplicate) of the fouled membrane sheets by physical scrapping. Dry foulants were obtained through freeze-drying. The recovered foulants were weighed, and the mass per unit surface area of the fouled membrane was calculated.

**Loss on ignition (LOI) test** Accurately weighed quantities (approximately 1000 mg, performed in triplicate) of the lyophilized foulants were subjected to ignition at 550 °C in a muffle furnace for 6 h. The LOI percentage was then calculated (Khan et al. 2014, Khan et al. 2013).

**Organic foulant extraction (Wang and Tang 2011) and analysis** Membrane samples (200 cm<sup>2</sup>, performed in triplicate) were used for foulant extraction. A 400-mL mixed solution containing 10 mM ethylenediaminetetraacetic acid (EDTA) and 2.5 mM sodium dodecyl sulfonate at pH = 12.0 was used for foulant extraction. Mild sonication (30 min) was employed after 24 h soaking of the samples in the extraction solution. Thereafter, the contents of the crude oil and APAM in the foulants were quantified by the methods described in the “Water quality characterization” section.

### Analytical methods

The molecular weight (MW) distributions of the organics in the feed and foulants were measured by high-performance size exclusion chromatography (LC-10CE, Shimadzu, Japan). Fourier transform infrared (FTIR) spectra of the lyophilized foulants were obtained with a potassium bromide pellet using an FTIR spectrometer (Nicolet 5700, Thermo Scientific,

USA). Measurements were conducted in the range of 4000–400 cm<sup>−1</sup> at a spectrum resolution of 4 cm<sup>−1</sup> using 32 scans for both the background and sample. Accurately weighed amounts of the ashed foulants (approximately 100 mg, performed in triplicate) were subjected to microwave digestion. After digestion, the transparent solution was obtained and diluted with ultrapure water. The dilution was then analyzed via ICP-OES for its concentrations of inorganic elements. The detailed sample preparation procedures are disclosed in Fig. S3. The crystal types of the foulants were characterized using XRD (D8 Advance, Bruker, Germany). The chemical compositions of the foulants were analyzed by X-ray photoelectron spectroscopy (XPS, PHI-5000C ESCA system, Perkin Elmer, USA) using Mg K $\alpha$  as the radiation source ( $h\nu = 1253.6$  eV).

## Results and discussion

### Performance

The water quality parameters of the feed and permeate from the NF facility are presented in Table 1. The ranges are shown in Table 1 for seven randomly selected water samples during long-term operation. Compared with that of the feed, the pH value of the permeate decreased. Normally, the NF membrane rejected multivalent cations (such as Mg<sup>2+</sup>, Ca<sup>2+</sup>, Fe<sup>3+</sup>, and Al<sup>3+</sup>) with a high efficiency (see Table 2), which caused an increase of protons in the permeate base on the electrical equilibrium (Luo & Wan 2013, Mazzoni et al. 2007). Then, the pH of the permeate decreased. The TDS in the permeate was below 1000 mg/L, meeting the standard for reinjection water quality (Zhang et al. 2015). The rejection rates of the NF membrane for monovalent ions (e.g., Na<sup>+</sup>, K<sup>+</sup>) were above 90%, whereas the rejection rates of the NF membrane for multivalent cations (such as Mg<sup>2+</sup>, Ca<sup>2+</sup>, Fe<sup>3+</sup>, and Al<sup>3+</sup>) were close to 100%. APAM was not detected in the permeate, indicating that the macromolecular APAM could not easily pass through the NF membrane pores that were smaller than 1 nm (Kumar & Pal 2014, Mo et al. 2012). The content of crude oil in the permeate was in the range of 0.25 to 0.31 mg/L, suggesting that alkanes with low molecular weight (Esquinas et al. 2017) passed through the NF membrane pores.

The long-term flux variations at the NF facility are shown in Fig. 2a. From 0 to 480 days, the average flux at the NF facility decreased from 4.0 to approximately 3.0 L/(m<sup>2</sup> h MPa), indicating that chemically irreversible fouling of the NF membranes gradually enhanced. As shown in Fig. 2b, the long-term rejection performance of the NF facility was fairly stable. The permeate conductivity of the NF facility was in the range of 200–700  $\mu$ S/cm, which satisfied the standard for reinjection water quality (Zhang et al. 2015).

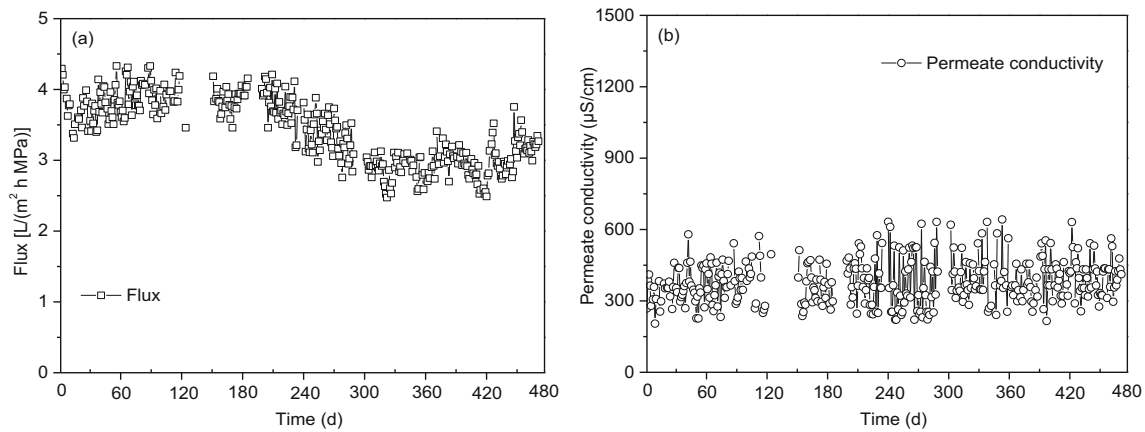


**Fig. 2** Long-term operational performance of the NF facility: variations in flux (a) and permeate (b) conductivity. The data shown in the figure are the average values for the total NF facility (including #1, #2, and #3 in Fig. 1)

**Efficiency comparison of the two cleaning modes**

Chemical cleaning is mandatory at the NF facility due to membrane fouling. Figure 3 shows the variations in the permeate flux of the NF facility after being cleaned by two cleaning modes. The acid/PL-007@PL-007/acid and PL-007/acid@acid/PL-007 cleaning procedures were conducted for facility #1 and facility #2 in Fig. 1, respectively, and the results are shown in Fig. 3a and b, respectively. As shown in Fig. 3a, the flux of facility #1 had no significant change and was still maintained at approximately 3.3 L/(m<sup>2</sup> h MPa) after acid/PL-007 cleaning, while after PL-007/acid cleaning, the flux of facility #1 obviously increased from 2.5 to 3.2 L/(m<sup>2</sup> h MPa). Similarly, as displayed in Fig. 3b, the flux of facility #2 significantly increased from 3.0 to 3.8 L/(m<sup>2</sup> h MPa) after PL-007/acid cleaning, while after acid/PL-007 cleaning, the flux of facility #2 only increased from 3.1 to 3.3 L/(m<sup>2</sup> h MPa). These results indicated that the cleaning efficiency of the PL-007/acid procedure was higher than that of the acid/PL-007 procedure. The reason for these differences in efficiency may be that the commercial cleaning agent (i.e.,

PL-007) contained sodium hydroxide and an anionic surfactant. Therefore, the alkaline environment could deprotonate the foulants (i.e., APAM) on the membrane surface and cause the fouling layer to become loose. Moreover, the anionic surfactant in the agent has a strong removal capacity for crude oil (Fletcher et al. 2015, Wang et al. 2014) on the membrane surface, which favors the exposure of inorganic foulants encapsulated by organics. Subsequent acid cleaning can improve the removal of such foulants.

Before ICP-OES analysis, the cleaning solutions from the two cleaning modes were subjected to microwave digestion. The ICP-OES analysis results are shown in Table 3. For the two cleaning modes, the contents of the inorganic elements in the acid solutions were higher than those in the PL-007 solutions, while the concentrations of organics (i.e., crude oil and APAM) in the PL-007 solutions were significantly higher than those in the acid solutions. These results indicated that the acid cleaning agent was more effective for the removal of inorganic foulants, while PL-007 was more effective for the removal of organic foulants. Additionally, the contents of inorganic elements (Mg, Ca, Fe, Al, and Si) in the acid cleaning solution

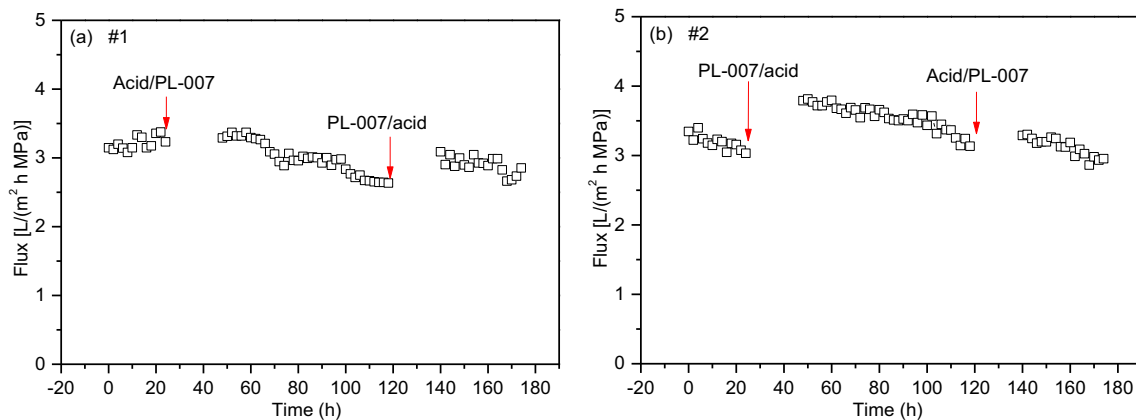


**Fig. 3** Efficiency comparisons of two cleaning modes: Acid/PL-007@PL-007/acid cleaning for facility #1 (a) and PL-007/acid@acid/PL-007 cleaning for facility #2 (b) in Fig. 1

**Table 3** Component analysis in the cleaning solutions for the two cleaning modes

Type of cleaning solutions	Mg	Ca	Fe	Al	Si	Crude oil	APAM
Acid/PL-007@PL-007/acid cleaning for facility #1							
Acid/PL-007							
Acid	0.23	1.35	2.32	0.52	3.01	2.53	59.17
PL-007	0.57	5.29	1.6	0.4	2.58	32.71	460.4
PL-007/acid							
PL-007	–	–	2.16	0.16	3.73	60	462.8
Acid	2.02	33.16	3.94	0.68	3.03	4.74	34.88
PL-007/Acid@acid/PL-007 cleaning for facility #2							
PL-007/acid							
PL-007	0.19	2.31	2.69	0.53	3.16	68.64	523.6
Acid	3.93	35.62	4.36	0.63	4.32	3.25	32.85
Acid/PL-007							
Acid	1.93	2.34	2.46	0.56	3.26	2.89	52.86
PL-007	0.86	6.96	1.89	0.35	2.89	40.26	476.3

The units for the contents in the table are all mg/L

from the PL-007/acid cleaning mode were significantly higher than those in the acid cleaning solution from the acid/PL-007 cleaning mode, which corroborated the abovementioned inference that PL-007 cleaning helped improve the effectiveness of the subsequent acid cleaning in the removal of inorganic foulants.

### Autopsy of fouled NF membranes

After frequent chemical cleaning, the nature of the residual foulants on the membrane surface is the key factor determining the magnitude of the membrane flux (Wang et al. 2014). Identification of the residual foulants on the membrane surface is crucial for a reasonable analysis of the fouling cause.

### SEM-EDX analysis

Representative SEM images of the fouled NF membranes collected from the plant are presented in Fig. 4a. The fouling layer almost completely covered the membrane surface, and the intrinsic “leaf-like” surface morphology of fully aromatic polyamide NF membranes (Li et al. 2014) was invisible. EDX elemental analysis of the bulged area of the fouling layer (Fig. 4b) showed that a range of elements, including Na, Mg, Ca, Fe, Al, and Si, were present in limited amounts. In the flat region of the fouling layer (Fig. 4c), slight signals for inorganic elements corresponding to Na, Ba, Ca, Fe, Al, and Si were observed. A cross-sectional image of the fouled membrane is exhibited in Fig. 4d. There were no discernible inorganic peaks detected in the EDX spectrum, indicating that inorganic fouling did not occur in the supporting layer. The EDX elemental analysis results of the fouled NF membranes are shown in Table 4.

### Fouling load

The fouling load of the fouled NF membranes is displayed in Fig. 5. The dry weight of the foulants after lyophilization was 940.8 mg/m<sup>2</sup>. The fouling loads of crude oil and APAM were 320.1 and 492.7 mg/m<sup>2</sup>, respectively. The analysis of organic/inorganic fractions by LOI measurement revealed that the foulants were mainly organic in nature (86.3%) and that the inorganic fraction of the foulants only accounted for 13.7% of the total mass; i.e., organic fouling was the main issue for the NF membranes.

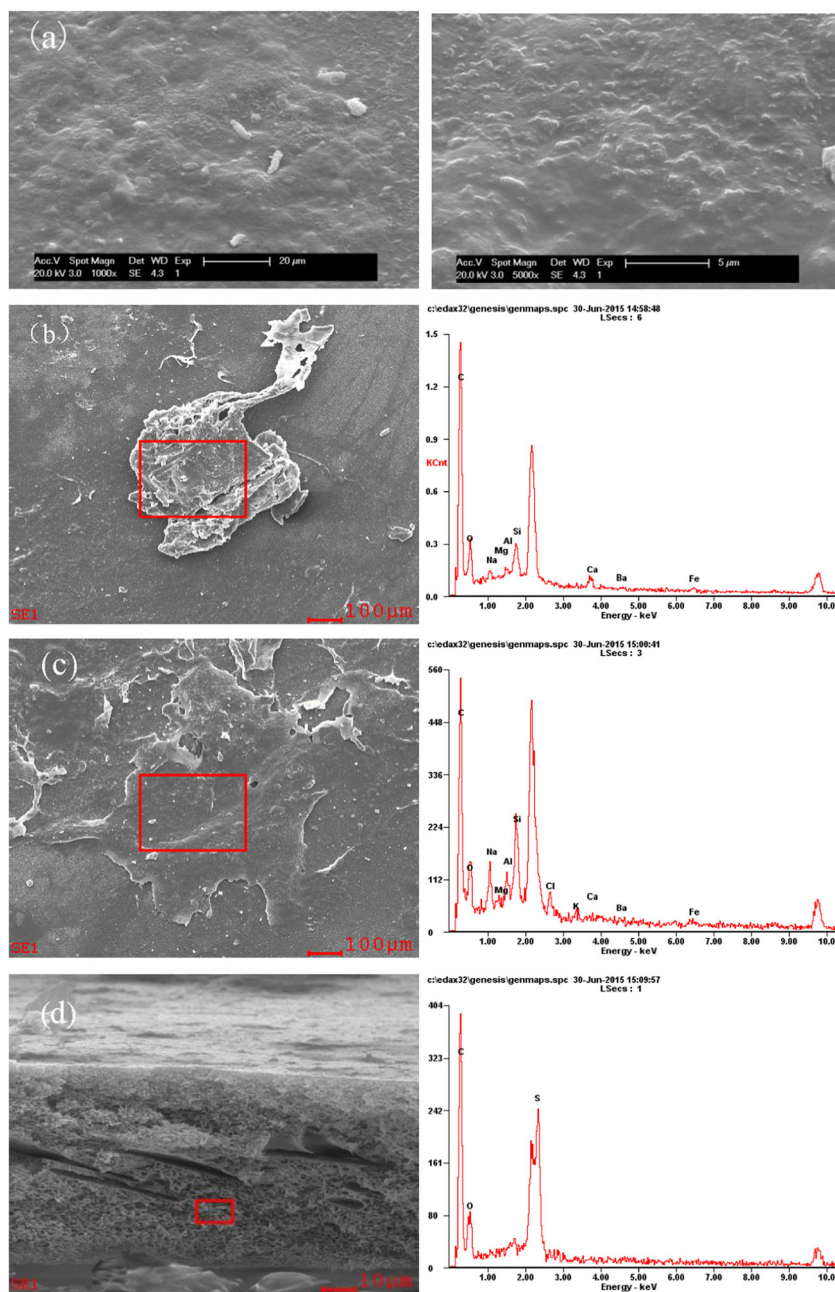
### Molecular weight distributions

The molecular weight distributions of the organics in the NF feed and the foulants are shown in Fig. 6. The molecular weight distributions of the organics in the feed and the foulants had peaks at approximately 600,000 Da and 2,000,000 Da, respectively. Accordingly, compared to the foulants with low molecular weight, the foulants with high molecular weight were prone to accumulation on the membrane surface. It can be concluded that the molecular weight of the organics in the NF feed played a crucial role in membrane fouling.

### Chemical analyses

A typical FTIR spectrum of the foulants isolated from the membrane surface is displayed in Fig. 7a. The peaks at 3250 and 1630 cm<sup>-1</sup> are representative of the –NH stretching vibration of amide II and the C=O stretching vibration of amide I, respectively, which are the characteristic bonds of APAM

**Fig. 4** SEM images and the corresponding EDX spectra of fouled membranes



(Guo et al. 2015). The absorption peaks at 2924, 2854, 1459, 1379, and 720  $\text{cm}^{-1}$  are related to the bonds in aliphatic hydrocarbons  $\text{CH}_3-(\text{CH}_2)_n-\text{CH}_3$  (where  $n$  is 3 or greater), indicating the existence of crude oil in the fouling layer (Meléndez et al. 2012). The prominent peak at 1042  $\text{cm}^{-1}$  can be assigned to the stretching vibration of Si–O bonds (Gorzalski & Coronell 2014, Tang et al. 2014), suggesting the occurrence of silica fouling.

Unlike the EDX spectrum analysis, the ICP-OES analysis can provide the average contents of inorganic elements in the fouling layer. The inorganic element contents from ICP-OES analysis are exhibited in Fig. 7b. The inorganic components of the foulants mainly consisted of Na, Mg, Ca, Fe, Al, and Si.

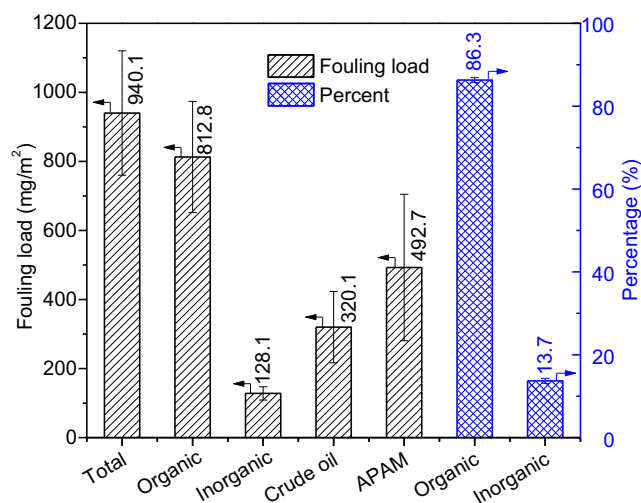
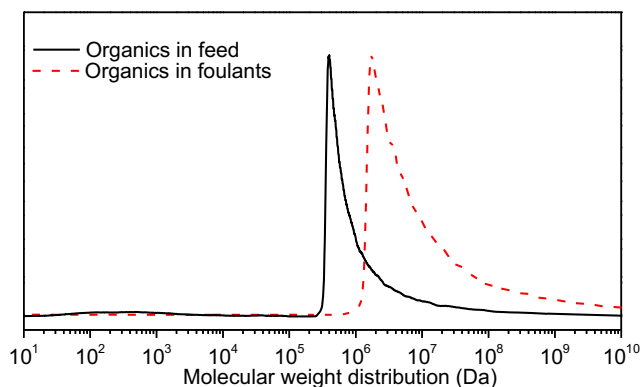
Compared to the other elements, Si occupied a relatively high level (39.62 mg/g) in the fouling layer, which was consistent with the EDX results. Although the contents of Al and Fe were relatively low in the feed (in the range of 0.08–0.21 mg/L and 0.45–0.83 mg/L, respectively), they accounted for higher proportions in the inorganic fraction than the divalent elements (i.e., Ca and Mg) did, which could be attributed to their stronger coordinating abilities with the carboxylate groups of the membrane surface and the APAM molecules relative to those of divalent ions (Mo et al. 2012), (Rivas et al. 2011). These results suggested that the removal of multivalent elements, particularly Al, Fe, and Si, is the key to controlling NF membrane fouling.

**Table 4** EDX elemental analysis results of the fouled membranes

Elements	Percent (%)		
	b	c	d
C	75.16	69.90	77.99
O	17.79	16.26	14.16
S	–	–	7.85
Na	1.18	2.88	–
K	–	0.49	–
Cl	–	1.28	–
Mg	0.18	–	–
Ca	1.54	0.51	–
Ba	–	1.45	–
Fe	1.29	1.69	–
Al	0.41	1.19	–
Si	2.46	4.35	–

The XRD spectrum of the foulants after freeze-drying is presented in Fig. 7c. The  $2\theta$  peaks at  $27.3^\circ$ ,  $31.7^\circ$ ,  $45.5^\circ$ ,  $53.8^\circ$ ,  $56.4^\circ$ ,  $66.2^\circ$ , and  $75.2^\circ$  are the characteristic peaks of NaCl. The  $2\theta$  peaks at  $20.8^\circ$ ,  $26.7^\circ$ ,  $36.5^\circ$ ,  $39.5^\circ$ ,  $40.3^\circ$ ,  $42.5^\circ$ ,  $45.8^\circ$ ,  $50.1^\circ$ ,  $59.9^\circ$ , and  $68.1^\circ$  are the characteristic peaks of  $\text{SiO}_2$  (Zhou et al. 2015). These results showed that the inorganic crystals in the foulants were mainly composed of NaCl and  $\text{SiO}_2$ . Figure 7d shows the XPS Si2p3 narrow spectrum of the foulants. According to the XPS standard spectra, the binding energy at 103.9 eV corresponded to the characteristic peak of  $\text{SiO}_2$  (Zhou et al. 2015). Accordingly, Si existed in the form of  $\text{SiO}_2$  in the fouling layer. The peaks of other inorganic elements could not be identified as a result of their low contents.

Based on the above discussion, the fouling mechanisms of NF membranes in oil-field wastewater treatment were proposed and are presented in Fig. 8. Hydrophilic APAM, with a high molecular weight, can attach to the polyamide NF

**Fig. 5** Fouling load of fouled NF membranes**Fig. 6** Molecular weight distributions of the organics in the feed and foulants

membrane surface by hydrogen bonds and coordination bonds with multivalent-ion (i.e., Ca, Fe, and Al)-bridging carboxylate groups (Li & Elimelech 2004, Liu et al. 2016b). Meanwhile, these bonds can also occur among APAM molecules, which makes the gel layer denser and more compact (Zhang et al. 2015). Moreover, hydrophobic crude oil containing alkanes may adhere to the benzene rings of polyamide membrane surfaces and the nonpolar hydrocarbon chains of APAM molecules through hydrophobic attractions, resulting in a mixture of crude oil and APAM molecules in the fouling layer. In addition, the accumulated APAM molecules could act as sites for silica deposition (Gorzalski & Coronell 2014) and further aggravate membrane fouling.

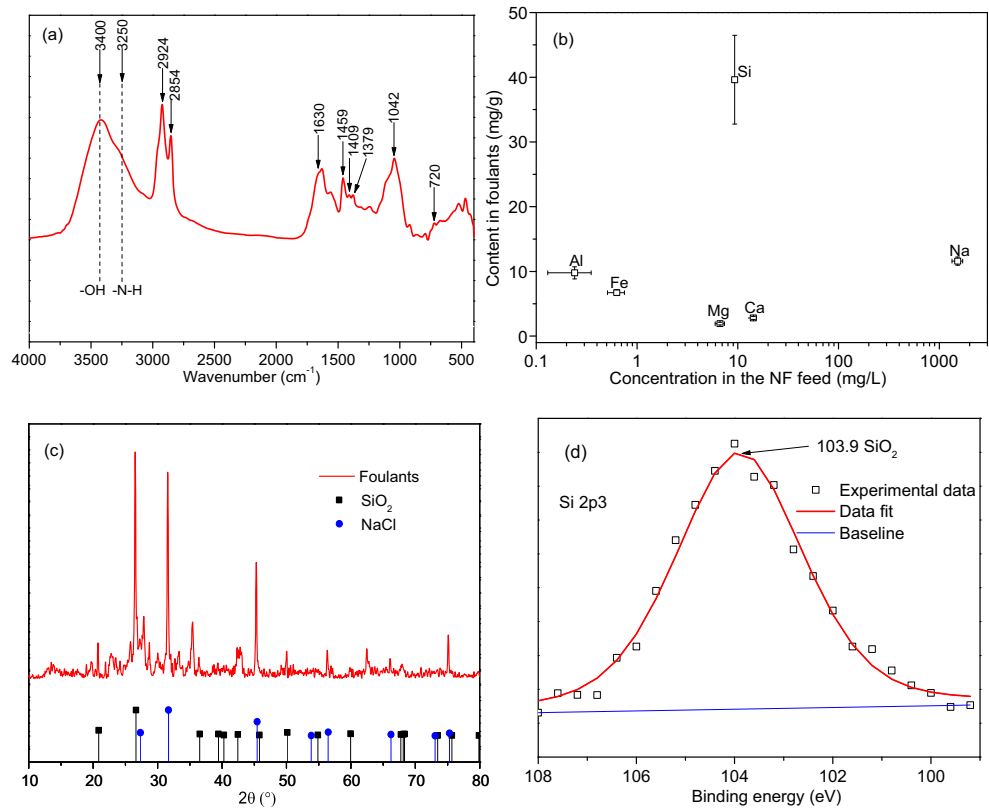
## Implications and recommendations

Although the implemented UF pretreatment process (Fig. S1) was targeted at reducing the amount of APAM and crude oil in the NF feed, it was not effective in removing multivalent elements and silica. Additionally, a small fraction of APAM and crude oil still passed through the UF barriers, subsequently resulting in severe NF membrane fouling in conjunction with multivalent elements and silica. Nevertheless, there is no specific pretreatment aimed at Al, Fe, and Si removal. Therefore, the optimization of existing pretreatment strategies or the development of cost-effective procedures to guarantee the elimination of Al, Fe, and Si from the feed of the NF facility is essential.

The results achieved in this work provide an important data basis for a further study on the NF membrane fouling mechanism in oil-field wastewater desalination. In particular, the meaningful findings in this study are as follows: the differences of the molecular weight of organics in the feed and on the membrane surface (see Fig. 6), the main organic components (APAM and crude oil) in the foulants, and the co-existence of APAM and inorganic elements (such as Na, Mg, Ca, Fe, Al) and  $\text{SiO}_2$  in the fouling layer.



**Fig. 7** Chemical analyses of the foulants: FTIR spectrum (a), ICP-OES analysis (b), XRD spectra (c), and XPS Si 2p3 narrow spectrum (d)



Future efforts should focus on the NF membrane fouling behavior caused by APAM with different molecular weights, the combined organic fouling characteristics of the NF membrane caused by APAM and crude oil, and the influence of the interaction between APAM and metal ions or colloid SiO<sub>2</sub> on the fouling behavior of the NF membrane.

### Conclusions

The long-term performance monitoring of an NF facility and comprehensive analysis of the fouled NF membranes at an oil-field wastewater desalination plant were conducted. The flux of the NF facility decreased gradually during

long-term operation due to membrane fouling. The efficiency of PL-007/acid cleaning was better than that of acid/PL-007 cleaning based on the flux recovery. The autopsy results showed that the organic foulants on the fouled NF membrane surface were mainly composed of APAM and crude oil and accounted for 86.3% of the total foulants in terms of dry weight. The organics with high molecular weight were more prone to accumulation on the membrane surface than those with low molecular weight. In the fouling layer, the inorganic elements mainly included Mg, Ca, Fe, Al, and Si, with Si existing in the form of SiO<sub>2</sub>. According to the autopsy results, organic fouling combined with inorganics was responsible for the flux decline in the NF membranes.

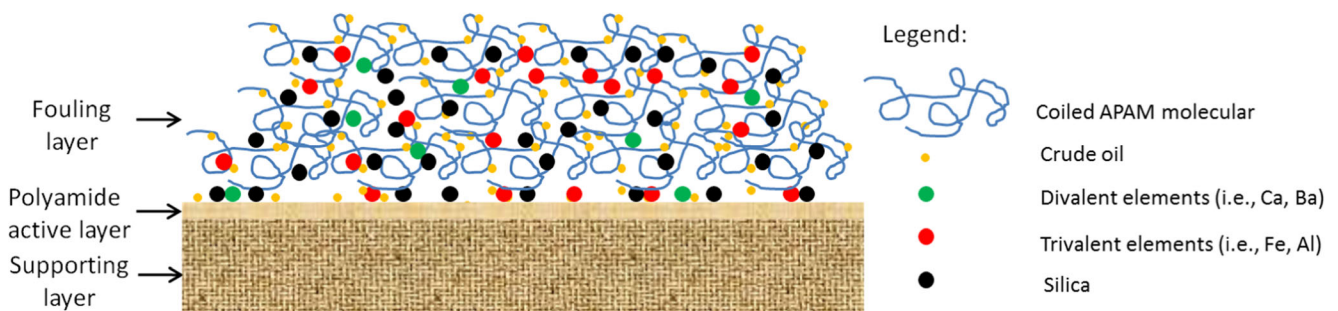


**Fig. 8** Proposed fouling mechanisms of the NF membranes fouled by oil-field wastewater

**Funding information** This research was financially supported by the Natural Science Foundation of Shandong Province (ZR2018BEE040) and the Scientific Research Project of Nanyang Normal University (2018ZX022).

## References

- Alzahrani S, Mohammad AW, Hilal N, Abdullah P, Jaafar O (2013) Identification of foulants, fouling mechanisms and cleaning efficiency for NF and RO treatment of produced water. *Sep Purif Technol* 118:324–341
- Antony A, Low JH, Gray S, Childress AE, Le-Clech P, Leslie G (2011) Scale formation and control in high pressure membrane water treatment systems: a review. *J Membr Sci* 383:1–16
- Asatekin A, Mayes AM (2009) Oil industry wastewater treatment with fouling resistant membranes containing amphiphilic comb copolymers. *Environ Sci Technol* 43:4487–4492
- Cakmakci M, Kayaalp N, Koyuncu I (2008) Desalination of produced water from oil production fields by membrane processes. *Desalination* 222:176–186
- Esquinas N, Rodriguez-Valdes E, Marquez G, Gallego JLR (2017) Diagnostic ratios for the rapid evaluation of natural attenuation of heavy fuel oil pollution along shores. *Chemosphere* 184:1089–1098
- Fletcher PD, Savory LD, Woods F, Clarke A, Howe AM (2015) Model study of enhanced oil recovery by flooding with aqueous surfactant solution and comparison with theory. *Langmuir* 31:3076–3085
- Gorzalski AS, Coronell O (2014) Fouling of nanofiltration membranes in full- and bench-scale systems treating groundwater containing silica. *J Membr Sci* 468:349–359
- Guo H, You F, Yu S, Li L, Zhao D (2015) Mechanisms of chemical cleaning of ion exchange membranes: a case study of plant-scale electro dialysis for oily wastewater treatment. *J Membr Sci* 496:310–317
- Gur-Reznik S, Katz I, Dosoretz CG (2008) Removal of dissolved organic matter by granular-activated carbon adsorption as a pretreatment to reverse osmosis of membrane bioreactor effluents. *Water Res* 42:1595–1605
- Han G, de Wit JS, Chung T-S (2015) Water reclamation from emulsified oily wastewater via effective forward osmosis hollow fiber membranes under the PRO mode. *Water Res* 81:54–63
- Kang GD, Cao YM (2012) Development of antifouling reverse osmosis membranes for water treatment: a review. *Water Res* 46:584–600
- Khan MT, Manes CLD, Aubry C, Croue JP (2013) Source water quality shaping different fouling scenarios in a full-scale desalination plant at the Red Sea. *Water Res* 47:558–568
- Khan MT, Busch M, Molina VG, Emwas AH, Aubry C, Croue JP (2014) How different is the composition of the fouling layer of wastewater reuse and seawater desalination RO membranes? *Water Res* 59:271–282
- Kumar R, Pal P (2014) Membrane-integrated hybrid system for the effective treatment of ammoniacal wastewater of coke-making plant: a volume reduction approach. *Environ Technol* 35:2018–2027
- Lai CH, Chen YH, Yeh HH (2013) Effects of feed water quality and pretreatment on NF membrane fouling control. *Sep Sci Technol* 48:1609–1615
- Li QL, Elimelech M (2004) Organic fouling and chemical cleaning of nanofiltration membranes: measurements and mechanisms. *Environ Sci Technol* 38:4683–4693
- Li Q, Song J, Yu H, Li Z, Pan X, Yang B (2014) Investigating the microstructures and surface features of seawater RO membranes and the dependencies of fouling resistance performances. *Desalination* 352:109–117
- Li M, Romero-Zeron L, Marica F, Balcom BJ (2017) Polymer flooding enhanced oil recovery evaluated with magnetic resonance imaging and relaxation time measurements. *Energy Fuel* 31:4904–4914
- Liu G, Yu S, Yang H, Hu J, Zhang Y, He B, Li L, Liu Z (2016a) Molecular mechanisms of ultrafiltration membrane fouling in polymer-flooding wastewater treatment: role of ions in polymeric fouling. *Environ Sci Technol* 50:1393–1402
- Liu G, Yu S, Yang H, Hu J, Zhang Y, He B, Li L, Liu Z (2016b) Molecular mechanisms of ultrafiltration membrane fouling in polymer-flooding wastewater treatment: role of ions in polymeric fouling. *Environ Sci Technol* 50:1393–1402
- Luo J, Wan Y (2013) Effects of pH and salt on nanofiltration—a critical review. *J Membr Sci* 438:18–28
- Mazzoni C, Bruni L, Bandini S (2007) Nanofiltration: role of the electrolyte and pH on desalination performances. *Ind Eng Chem Res* 46:2254–2262
- Meléndez LV, Lache A, Orrego-Ruiz JA, Pachón Z, Mejía-Ospino E (2012) Prediction of the SARA analysis of Colombian crude oils using ATR–FTIR spectroscopy and chemometric methods. *J Pet Sci Eng* 90–91:56–60
- Mo YH, Tiraferri A, Yip NY, Adout A, Huang X, Elimelech M (2012) Improved antifouling properties of polyamide nanofiltration membranes by reducing the density of surface carboxyl groups. *Environ Sci Technol* 46:13253–13261
- Mondal S, Wickramasinghe SR (2008) Produced water treatment by nanofiltration and reverse osmosis membranes. *J Membr Sci* 322:162–170
- Ochando-Pulido JM, Rodriguez-Vives S, Hodaifa G, Martinez-Ferez A (2012) Impacts of operating conditions on reverse osmosis performance of pretreated olive mill wastewater. *Water Res* 46:4621–4632
- Ohno K, Matsui Y, Itoh M, Oguchi Y, Kondo T, Konno Y, Matsushita T, Magara Y (2010) NF membrane fouling by aluminum and iron coagulant residuals after coagulation–MF pretreatment. *Desalination* 254:17–22
- Phuntho S, Lotfi F, Hong S, Shaffer DL, Elimelech M, Shon HK (2014) Membrane scaling and flux decline during fertiliser-drawn forward osmosis desalination of brackish groundwater. *Water Res* 57:172–182
- Riahinezhad M, Romero-Zeron L, McManus N, Penlidis A (2017) Evaluating the performance of tailor-made water-soluble copolymers for enhanced oil recovery polymer flooding applications. *Fuel* 203:269–278
- Rivas BL, Pereira ED, Palencia M, Sanchez J (2011) Water-soluble functional polymers in conjunction with membranes to remove pollutant ions from aqueous solutions. *Prog Polym Sci* 36:294–322
- Tang F, Hu H-Y, Sun L-J, Wu Q-Y, Jiang Y-M, Guan Y-T, Huang J-J (2014) Fouling of reverse osmosis membrane for municipal wastewater reclamation: autopsy results from a full-scale plant. *Desalination* 349:73–79
- Wang Y-N, Tang CY (2011) Nanofiltration membrane fouling by oppositely charged macromolecules: investigation on flux behavior, foulant mass deposition, and solute rejection. *Environ Sci Technol* 45:8941–8947
- Wang Z, Ma J, Tang CY, Kimura K, Wang Q, Han X (2014) Membrane cleaning in membrane bioreactors: a review. *J Membr Sci* 468:276–307
- Zhang R, Shi W, Yu S, Wang W, Zhang Z, Zhang B, Li L, Bao X (2015) Influence of salts, anion polyacrylamide and crude oil on nanofiltration membrane fouling during desalination process of polymer flooding produced water. *Desalination* 373:27–37
- Zhao L, Ho WSW (2014) Novel reverse osmosis membranes incorporated with a hydrophilic additive for seawater desalination. *J Membr Sci* 455:44–54
- Zhao HY, Qiu S, Wu LG, Zhang L, Chen HL, Gao CJ (2014) Improving the performance of polyamide reverse osmosis membrane by incorporation of modified multi-walled carbon nanotubes. *J Membr Sci* 450:249–256
- Zhou L, Xia S, Alvarez-Cohen L (2015) Structure and distribution of inorganic components in the cake layer of a membrane bioreactor treating municipal wastewater. *Bioresour Technol* 196:586–591